Hydrophobic/oleophilic nanofibrous membranes for oil/water separation by suspension electrospinning and PDMS photo-induced grafting

Journal of Membrane Science 734 (2025) 124457

Contents lists available at ScienceDirect

Journal of Membrane Science

journal homepage: www.elsevier.com/locate/memsci

Hydrophobic/oleophilic nanofibrous membranes for oil/water separation by suspension electrospinning and PDMS photo-induced grafting

Jessica Alexandra Talamo Ruiz, Parnian Kianfar, Sara Dalle Vacche, Roberta Bongiovanni, Alessandra Vitale *

Department of Applied Science and Technology, Politecnico di Torino, Corso Duca degli Abruzzi 24, 10129, Torino, Italy

ARTICLE INFO

Keywords:
Polydimethylsiloxane
SBR latex
Green electrospinning
Membrane functionalization
Thiol-ene grafting

ABSTRACT

This study presents a simple and efficient method for fabricating rubber nanofibrous membranes for oil/water separation. The process involves suspension electrospinning of styrene-butadiene rubber (SBR) latex, followed by photo-induced crosslinking to ensure insolubility and shape stability, as well as photo-induced grafting to achieve durable hydrophobicity and oleophilicity. A vinyl-terminated polydimethylsiloxane (PDMS) functionalizing agent was grafted onto the nanofibers through a thiol-ene reaction, under various functionalization conditions (e.g., solution concentrations and immersion times). FT-IR analyses confirmed successful functionalization: the resulting PDMS-grafted membranes exhibited well-defined, uniform, cylindrical fibers with an average diameter of 439 nm, a high surface area, and a structure composed of partially fused rubber nanoparticles. Contact angle measurements demonstrated stable hydrophobicity (water contact angle of 123° after 30 min, water-in-oil contact angle of 122° after 24 h) and strong oleophilicity (oil contact angle <10°). The membranes effectively separated oil from water, achieving an average separation efficiency of 99.3 % and an oil flux of 988 L m^{-2} h^{-1} after 20 filtration cycles of an oil/water mixture. These results highlight the potential of hydrophobic/oleophilic PDMS-functionalized rubber nanofibrous membranes for oily wastewater treatment and environmental remediation applications.

1. Introduction

The constant growth of industrial activities has led to a reduction in the availability of clean water sources worldwide due to the serious pollution generated by waste products. Indeed, oil is a severe pollutant for any aqueous system, as it is capable of covering large areas of clean water in a very easy and fast way. Metallurgy and food processing contribute to water pollution, but the petrochemical and oil industries are undoubtedly among the most significant sources [1]. Even though oily wastewater represents a hazard to human health and to several levels of the environment [2], conventional techniques for the treatment of oily wastewater currently available are often limited by particular disadvantages. In fact, techniques such as flotation and coagulation [3], gravity separation [4], flocculation [5], absorption [6] and biological [4] and electrochemical [7] methods are often demanding in terms of energy and financial capital, require considerable space and personnel to operate the treatment facilities or present low efficiencies. The search for alternative techniques for the treatment of oily wastewater has led to the use of innovative materials capable of separating oil and water with a reduced environmental and economic impact. Among the approaches proposed, the production of membranes with tunable surface characteristics has emerged, since it demands moderate operating temperatures and usually does not require the use of toxic agents [8]. Specifically, efforts are being focused on generating selective wettability by producing superoleophilic and superhydrophobic membranes [9–11].

Electrospinning is a versatile technique for fabricating nonwoven membranes composed of fine submicrometric fibers from polymer solutions or melts under high electrostatic forces [12,13]. It also enables nanofiber functionalization during or after fabrication, allowing the incorporation of functional agents such as drugs, enzymes, metal nanoparticles, and catalysts [14,15]. Electrospun nanofibrous membranes offer significant advantages for oil/water separation, including high porosity, good pore connectivity, scalable fabrication, and large variety of materials to be processed [16,17]. Among these, rubber polymeric materials stand out due to their elasticity, extensibility,

* Corresponding author.
E-mail address: alessandra.vitale@polito.it (A. Vitale).

https://doi.org/10.1016/j.memsci.2025.124457
Received 31 March 2025; Received in revised form 13 July 2025; Accepted 15 July 2025
Available online 17 July 2025

abrasion resistance, and resilience [18–21]. However, their low glass transition temperature (T_g) limits electrospinning applications, as cold flow over time leads to fiber thickening and structural collapse [22]. This issue can be addressed through chemical crosslinking, which stabilizes the fibrous structure by restricting polymer chain mobility. In a recent work [22], we proposed a sustainable approach to prepare ultrafine, shape-stable rubber fibrous membranes by suspension electrospinning [23] of a styrene-butadiene rubber (SBR) latex, followed by thiol-ene photo-induced crosslinking under ambient conditions. A small quantity of an easily electrospinnable water-soluble polymer (specifically polyethylene oxide, PEO) was used as template polymer and could eventually be removed from the nanostructured membrane by a simple water treatment. A multifunctional thiol crosslinker and a suitable photo-initiating system were incorporated into the latex to enable rapid and efficient thiol-ene photo-induced crosslinking of the nanofibers through thiol addition to the SBR double bonds. The photo-induced chemical crosslinking ensured insolubility and structural stability, without compromising the nanofibrous morphology. It was also demonstrated [24] that by optimizing the thiol/ene stoichiometry and irradiation conditions, membranes with active thiol groups on their surface could be successfully produced.

For the application of such membranes as filters for wastewater treatment, they should exhibit a selective wettability, i.e., the ability to preferentially interact with specific liquids. Herein, to create hydrophobic and oleophilic membranes, electrospun SBR-based membranes were functionalized by chemically grafting a vinyl-terminated polydimethylsiloxane (PDMS) to the thiol groups on the surface of the membranes via a photo-induced thiol-ene reaction. Thiol-ene click reactions involve step-growth polymerization between multifunctional thiol and ene monomers, and can be efficiently initiated by UV irradiation [25]. These environmentally friendly reactions offer high efficiency, excellent tolerance to ambient oxygen and moisture, and proceed via a metal-free mechanism. Owing to these advantageous features, thiol-ene chemistry has attracted significant interest in membrane separation applications [26], including membrane fabrication, pre-functionalization, and grafting modifications. Such strategies have been successfully applied to a wide range of membrane materials, including polymers [27,28], cellulose [29], metals [30], and glass [31].

However, to the best of our knowledge, only a few studies have reported photo-induced thiol-ene modifications of membranes produced by electrospinning [32,33]. In this work, thiol-ene chemistry is employed both to ensure the insolubility and shape stability of the electrospun membrane through crosslinking, and to impart durable hydrophobicity and oleophilicity through surface grafting. Specifically, PDMS, a highly hydrophobic polymer characterized by a low glass transition temperature (<−120 °C) and low surface energy [34,35], was selected as the functionalizing agent to enhance and stabilize surface hydrophobicity. This modification prevents wetting by polar solvents such as water while allowing oil to permeate the membrane.

2. Materials and methods

2.1. Materials

A SBR latex, Elastolan S19 provided by RESCOM srl, was used as the main material to produce electrospun membranes. It is a 50 wt% aqueous dispersion of SBR copolymer (100–200 nm particle size) with a T_g of 6 °C and a viscosity of 300 cP s at 25 °C. PEO with a molecular weight (M_w) of 1,000,000 g mol^{-1}, purchased from Sigma-Aldrich, was used as template polymer for the electrospinning of the SBR latex. In order to promote the photo-induced cross-linking reaction of the SBR membranes, a photoinitiating system was added. A mixture of diphenyl (2,4,6-trimethylbenzoyl) phosphine oxide (TPO) and 2-hydroxy-2-methyl-1-phenyl-propan-1-one (Darocur 1173) was used. Both photoinitiators were provided by Sigma-Aldrich. In addition, trimethylolpropane tris(3-mercaptopropionate) (TRIS), a trifunctional thiol (-SH) monomer (Sigma-Aldrich), was used as crosslinking agent. A bifunctional vinyl terminated polydimethylsiloxane (PDMS, M_w: 28000 g mol^{-1}, vinyl: 0.18–0.26 wt%, 0.07–0.10 eq kg^{-1}, viscosity at 25 °C: 1000 cSt, density: 0.97 g mL^{-1}), supplied by Gelest Inc, was used as the functionalizing agent. All other chemicals were provided by Sigma-Aldrich. The chemical structure of the main materials used is reported in Fig. S1 of the Supporting Information.

2.2. Production of the rubber nanofibrous membranes

The first step in the fabrication of the membranes consisted of preparing the electrospinning SBR/PEO mixture. A primary aqueous solution of PEO at 5 wt% was prepared and magnetically stirred overnight at room temperature. SBR latex was then mixed with the PEO aqueous solution previously obtained, using an SBR/PEO mass ratio of 10:3, and the mixture was magnetically stirred for 2 h at room temperature. Then, the photoinitiating system (i.e., TPO dissolved in Darocur 1173 with a 1:1 mass ratio) was added to the mixture at 1 wt% with respect to SBR and the mixture was magnetically stirred for 15 min at room temperature. Finally, TRIS was added at 10 wt% with respect to SBR and the mixture was magnetically stirred for 5 min at room temperature. The electrospinning of the SBR/PEO mixture was performed by an E-fiber system (SKE Research Equipment) with a horizontal configuration. The main applied settings were: flow rate of 0.35 mL/h; diameter of the needle of 1 mm; working distance between the two electrodes of 15 cm; voltage ranging from 13 to 17 kV; temperature ranging from 16 to 24 °C and relative humidity ranging from 30 to 50 %. A plane stationary collector, covered with aluminum foil as substrate, was used. In some cases, a polytetrafluoethylene (PTFE) mesh or a polypropylene (PP) film was placed on the aluminum foil to facilitate the removal of the membrane from the substrate. The deposition of the fibers was carried out for 60–90 min for the production of each membrane. After electrospinning, the mats were carefully removed from the aluminum foil to obtain free-standing membranes.

After production, the samples were irradiated by UV light using a high-pressure mercury-xenon lamp with an optical fiber LIGHTNING-CURE Spot Light source LC8, Hamamatsu. To determine the appropriate intensity, the UV radiometer Power Puck® II from EIT® Instrument Markets was used. The membranes were irradiated at ambient conditions with an intensity of around 32 mW cm^{-2} for 5 min to promote the thiol-ene photoinduced crosslinking process. In order to remove the PEO present in the structure, obtaining SBR-based membranes [22], the samples were immersed in distilled water for 24 h and then dried for 5 h in air, allowing water evaporation.

2.3. Membranes functionalization

Once dried, the SBR-based membranes were subjected to surface functionalization using the PDMS monomer. In particular, the samples were immersed in a PDMS solution: three different concentrations of PDMS in toluene (i.e., 2, 5 and 10 wt%) and two different immersion times (i.e., 1 and 30 min) were used. Table 1 reports the experimental conditions employed for the grafting and the corresponding sample name. After removal from the solution, the membranes were dried using a compressed air gun. Subsequently, they were subjected to UV light irradiation (on one side) using the same instrument as described in the previous section with an intensity of 32 mW cm^{-2} for 5 min. The membranes were then washed for 1 min in toluene, in order to remove the monomer that did not react. Finally, they were left to dry in air for 24 h.

Using a digital micrometer, it was possible to measure the thickness of the functionalized membranes in at least five different spots. By calculating the average of these measurements, a range of 25–50 μm of thickness was measured.

Table 1
Experimental conditions used for the photo-induced grafting of the electrospun membranes and list of the samples investigated.

Sample	Sample name	PDMS concentration (wt.%)	Immersion time (min)
Photo-crosslinked SBR electrospun membranes	EM	–	–
PDMS-functionalized photo-crosslinked SBR electrospun membranes	EM-PDMS-2 %-1′	2	1
	EM-PDMS-2 %-30′	2	30
	EM-PDMS-5 %-1′	5	1
	EM-PDMS-5 %-30′	5	30
	EM-PDMS-10 %-1′	10	1
	EM-PDMS-10 %-30′	10	30

2.4. Characterization methods

The chemical structure and composition of the membranes were investigated through Fourier Transform Infrared (FT-IR) spectroscopy by using a Nicolet™ iS50 spectrometer (Thermo Fisher Scientific Inc., Waltham, MA, USA) and the results were analyzed using the Omnic™ software. Spectra were collected in attenuated total reflectance (ATR) mode in the spectral range of 4000–400 cm^{-1}, with an accumulation of 32 scans at a resolution of 4 cm^{-1}.

The morphology of the nanofibrous membranes was analyzed by means of the Supra 40 Field Emission Scanning Electron Microscopy (FE-SEM), ZEISS. Prior to analysis, the samples were coated through cathodic sputtering with a Quorum Q150T ES sputter coater in order to create a thin film of Pt of approximately 10 nm. Fiber diameters, surface porosity (i.e., the ratio of pore area to the total sample area), and average pore area were measured using ImageJ software by analyzing the FE-SEM images. Porosity analysis was performed by converting the images to binary format and applying a threshold to distinguish the pores. An energy-dispersive X-ray (EDX) probe using an Oxford liquid-N_2 cooled Si(Li) detector was used on the FE-SEM to analyze the chemical composition of the samples.

Concerning the wettability behavior of the membranes, different tests were performed to measure the contact angle using a FTA1000C Drop Shape Instrument (First Ten Angstroms), at room temperature with the sessile drop technique. Water and hexadecane (oil), with surface tensions of 72.1 mN m^{-1} and 28.1 mN m^{-1}, respectively, were used as probe liquids. Measurements were repeated at least in four different spots on the same membrane: the mean value and the error were calculated. Contact angle values were determined by the FTA32 software. For both water and hexadecane contact angles, the evolution of the deposited drop of the testing liquid on the surface of the membranes was recorded as a function of time (up to 30 min). Moreover, the contact angle of a drop of water on the functionalized membranes immersed in hexadecane (water-in-oil contact angle) and of a drop of hexadecane on the membranes immersed in water (oil-in-water contact angle) was measured. In this case, a transparent container was filled with oil or water respectively, the membrane was attached to a sample holder which in turn was fixed to the container and then the drop of the second liquid was deposited using a glass micropipette. Measurements were taken immediately after depositing the drop of the liquid on the membrane, and after 30 min and 24 h from deposition. To further assess the wettability behavior of the functionalized membranes the contact angle of silicon oil, soybean oil and mineral oil was studied as a function of time (up to 30 min).

To evaluate the effectiveness of the membranes for oil/water separation, a microfiltration system consisting of a Büchner flask, a Büchner funnel with a guko's conical silicone seal, a stainless-steel mesh, a PTFE gasket and a graduated cylinder was used. The components were fixed together using an anodized aluminum clamp to ensure the stability of system. A detailed schematic representation of the filtration system used is illustrated in Fig. S2 of the Supporting Information. For the filtration tests, water and hexadecane were used. Water was previously colored with a water-soluble and oil-insoluble blue dye in order to easily distinguish the presence of both liquids. The membrane samples were positioned on the stainless-steel mesh, ensuring full coverage of the filtration area. Subsequently, the PTFE gasket and the graduated cylinder were fixed with the clamp before proceeding to pour the liquids under study.

The initial phase of the analysis of the membranes performance consisted in testing the penetration capacity of oil (hexadecane) and dyed water individually, thus evaluating the wettability properties of the samples. The tests were carried out using only gravity as driven force. The liquid volume was measured using a graduated cylinder (10:1 mL, DIN -ln 20°, ±0.2 mL, Boro 3.3, Class A), while the weight was measured directly on the balance by making the necessary calibration adjustments. At the end of the test, the microfiltration system was disassembled to verify the integrity of the membrane used.

The second phase of the tests consisted in evaluating the membranes capacity to separate water and oil by quickly pouring both liquids in a 1:1 volumetric ratio and measuring the penetration of the liquids. In order to study the consistency of the separation efficiency of the membranes with time, 20 filtration cycles were repeated using the same membrane. To evaluate the reusability performance of the membranes, a cleaning protocol was applied after each oil/water separation cycle. The SBR electrospun membranes were first rinsed with isopropanol to effectively remove residual oil, followed by thorough rinsing with deionized water to eliminate any remaining solvent. Finally, the membranes were air-dried at room temperature to restore their original oil flux before reusing.

Finally, separation tests were performed using oil-in-water emulsions, which were prepared by stirring water and hexadecane in a 1:1 volumetric ratio, with 0.3 mg/mL sodium dodecyl sulfate, at 700 rpm for 15 min. Then, the emulsion was poured into the graduated cylinder, and the separation capacity of the membranes was analyzed.

Variations of the flux and efficiency expressions were used to quantitatively analyze the filtration system. In particular, the oil flux φ (L m^{-2} h^{-1}) was calculated using Equation (1):

$$\varphi = \frac{V}{ST} \tag{1}$$

where S is the effective area of the nanofibrous membrane positioned on the stainless-steel mesh (m^2), T is the separation time (h), and V is the permeate volume (L).

Furthermore, the quantity of oil before and after the filtration process was weighed and the percentage separation efficiency (η) was calculated according to Equation (2):

$$\eta = \frac{W_1}{W_0} \cdot 100\% \tag{2}$$

where W_0 and W_1 are the weight of oil before and after filtration, respectively.

3. Results and discussion

3.1. Photo-induced grafting of the electrospun membranes

In our previous work [22], we demonstrated a simple and efficient approach for obtaining shape-stable SBR nanofibrous membranes with a unique morphology and high surface area. This method involves suspension electrospinning of an SBR/PEO system containing a photo-initiating agent and a thiol crosslinker, followed by irradiation to trigger

a photo-induced thiol-ene crosslinking reaction. As the rubber nanofibers are made insoluble and morphologically stable, a subsequent water treatment removes the PEO template, without damaging the nanostructured rubber membranes. Moreover, photo-crosslinking hinders cold flow phenomena and the rubbery nanofibers maintain their shape over time. Herein, to better control the membranes surface wettability and optimize it for oil/water separation applications, the thiol groups of the crosslinker that remained available on the membranes surface after the crosslinking process [24] were used for functionalization. Specifically, a vinyl-terminated PDMS monomer was selected as the functionalizing agent. The membranes were immersed in a PDMS solution and irradiated after extraction, enabling the terminal vinyl groups of the PDMS monomer to react with the thiol groups of the nanofibers under light exposure. This process resulted in the formation of covalent bonds between the PDMS molecules and the SBR-based fibers through thiol-ene photo-induced chemical grafting. At the end of the fabrication process, functionalized free-standing, stable, flexible, and insoluble rubber nanofibrous membranes were obtained. A schematic representation of the entire fabrication and functionalization process is shown in Fig. 1.

For the photo-grafting, six different functionalization conditions were tested by using specific PDMS concentrations (2, 5, and 10 wt%) in toluene and immersion times of either 1 or 30 min (details in Table 1). The effects of these conditions on grafting efficiency and membrane properties were evaluated. It is important to underline that the electrospun fibers were not damaged by the solvent used for the functionalization step thanks to their crosslinked structure, while the surface chemistry changed. The chemical composition of the nanofibrous membranes was analyzed by ATR FT-IR spectroscopy, which confirmed the success of the grafting process. Fig. 2 presents the spectra corresponding to selected samples, while a complete set of spectra is available in Fig. S3 of the Supporting Information. The spectra of all functionalized membranes exhibited the characteristic absorption peaks of SBR (i.e., CH groups in the aromatic ring at 699 cm^{-1}, out-of-plane vibrations of the CH groups near the double bond at 910 cm^{-1} and at 962 cm^{-1}, C–C stretching in *cis*-butadiene units at 1029 cm^{-1}, CH vibrations in CH_2═CH- vinyl-butadiene at 1451 cm^{-1}, stretching of the C atoms in the aromatic ring at 1601 cm^{-1}), as well as of PDMS (i.e., CH_3 rocking and Si–C stretching in Si–CH_3 at 795 cm^{-1}, Si–*O*–Si stretching at 1020-1080 cm^{-1}, CH_3 deformation in Si–CH_3 at 1257 cm^{-1}, and asymmetric CH_3 stretching in Si–CH_3 at 2960 cm^{-1}). Furthermore, no significant differences were observed between the samples, regardless of immersion time

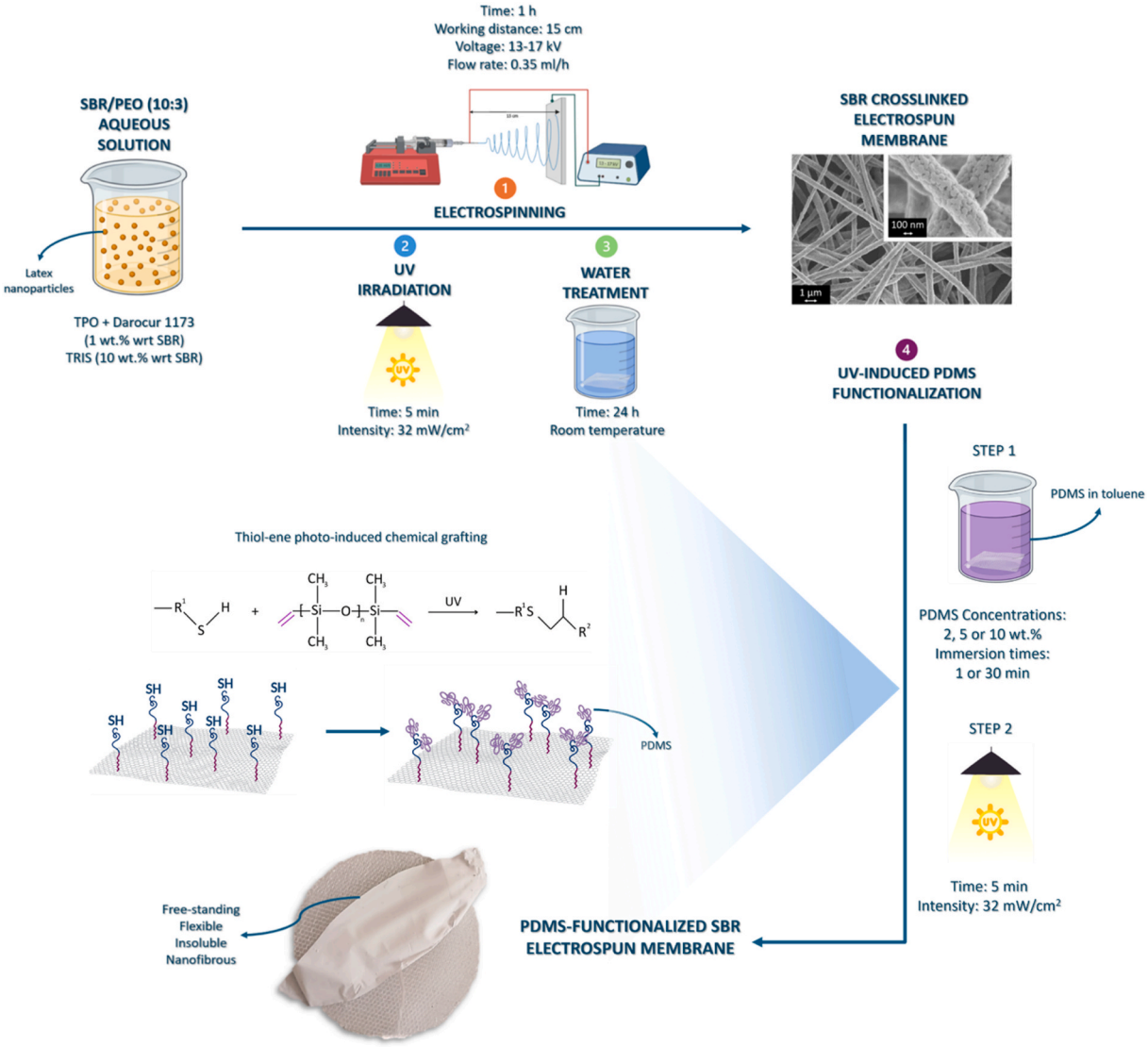

Fig. 1. Scheme of the process to prepare PDMS-grafted electrospun rubber membranes: electrospinning of SBR/PEO suspension, irradiation to promote the photo-induced crosslinking, water treatment to remove PEO template, and photo-induced functionalization with vinyl terminated PDMS. The thiol-ene grafting reaction is also reported.

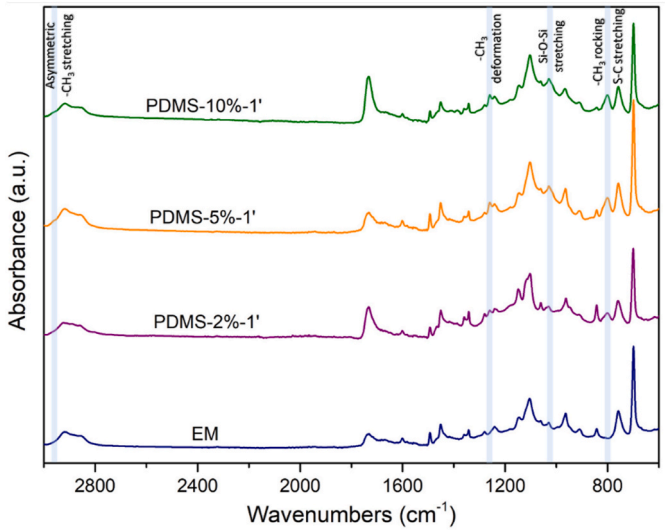

Fig. 2. ATR FT-IR spectra of the membranes before (EM) and after PDMS grafting with different solution concentrations: 2 wt% (PDMS-2 %-1′), 5 wt% (PDMS-5 %-1′), and 10 wt% (PDMS-10 %-1′).

or PDMS concentration, as shown in Fig. 2. These results suggest that PDMS was successfully chemically bonded onto the nanofibrous rubber membranes via photo-induced grafting, independent of the specific functionalization conditions applied. Moreover, FT-IR analyses were performed on both the upper and lower surfaces of the membrane, yielding identical spectra. This confirms that the functionalization was uniformly achieved across the entire membrane surface even if it was irradiated only on one side.

Contact angle measurements were performed to study the wetting behavior of the membranes. The evolution of the contact angle of water on the functionalized membranes was analyzed for 5 min. A non-functionalized membrane (EM) was investigated for comparison. As shown in Fig. 3, the reference membrane showed an initial contact angle of 75° immediately after droplet deposition. Although the system was crosslinked and morphologically stable [22], the contact angle was not stable over time: at the end of the test (i.e., after 5 min) it reached a value of about 10°. On the other hand, the membranes grafted with PDMS showed a completely different wettability behavior (Fig. 3). In particular, for the two systems photo-grafted with the 2 wt% PDMS solution

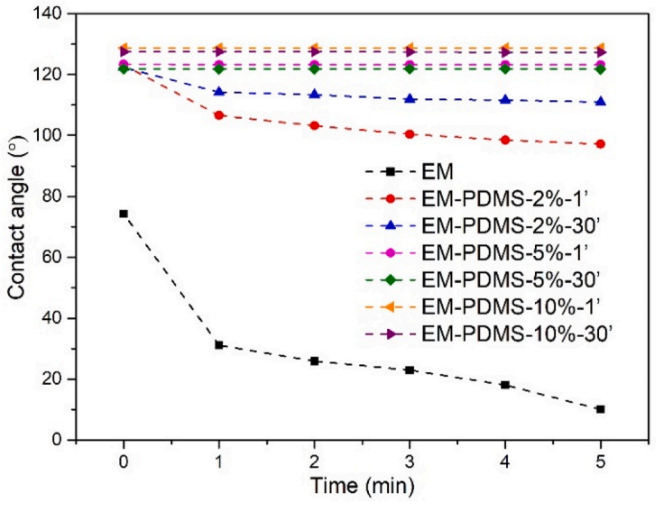

Fig. 3. Water contact angle as a function of droplet deposition time of the membranes before (EM) and after PDMS photo-induced grafting with different solution concentrations and immersion times.

(EM-PDMS-2 %-1′ and EM-PDMS-2 %-30′), an initial contact angle of 123° was recorded. With time, it decreased reaching a value of 97° and 111° for EM-PDMS-2 %-1′ and EM-PDMS-2 %-30′, respectively. The two systems photo-grafted with the 5 wt% PDMS solution (EM-PDMS-5 %-1′ and EM-PDMS-5 %-30′) displayed a contact angle of 123°, which remained completely stable over time. A similar result was observed for the membranes photo-grafted with the 10 wt% PDMS solution (EM-PDMS-10 %-1′ and EM-PDMS-10 %-30'), which showed a stable contact angle of 127°. Therefore, these results confirmed the success of the functionalization process of the fibers with PDMS in defined conditions: the chemically grafted hydrophobic polymer modified the wettability behavior of the membranes surface. Moreover, it can be concluded that the immersion time during the functionalization process is a parameter with negligible effect on the final wettability of the membranes. Whereas, the concentration of the PDMS solution used for the functionalization can affect the stability of the membranes hydrophobicity, which is guaranteed if the functionalizing agent has a concentration $\geq$5 wt%.

Thus, functionalization with a 5 wt% PDMS solution for a 1-min immersion was identified as the optimal process, ensuring the stable hydrophobicity required for oil/water separation, while minimizing both the amount of grafting agent used and the functionalization time. Although the EM-PDMS-10 % samples exhibited a slightly higher water contact angle compared to the EM-PDMS-5 % samples, all samples demonstrated complete wettability stability over time. Moreover, the 4° difference in water contact angle between EM-PDMS-5 %-1′ (123°) and EM-PDMS-10 %-1′ (127°) can be considered negligible and without significant effect on the membrane separation performance. Consequently, the sample EM-PDMS-5 %-1' was selected as the reference system for further characterization.

Once the hydrophobicity of the EM-PDMS-5 %-1' functionalized membranes was proven, the water contact angle tests were repeated for longer times (up to 30 min) to check the stability of the system, as needed for the real application in water filtration. As shown in Fig. 4, the wettability behavior of the PDMS-functionalized membrane was confirmed to be stable over time, maintaining a contact angle of 123° during the entire testing time (30 min). The non-functionalized membrane (EM) instead became superhydrophilic soon after the water droplet deposition. Thus, the functionalization resulted not only in an increase of the contact angle at time zero, but also in a significant improvement of the stability of the hydrophobicity over time.

The contact angle of oil (hexadecane) in air was also studied. For both non-functionalized (EM) and PDMS-functionalized (EM-PDMS-5 %-1') membranes, a distinct oleophilic behavior was observed. In fact, the initial value of the contact angle was 12° and 14° respectively, but within a few seconds the droplet spread completely, wetting the surface. In both cases, a contact angle lower than 10° was obtained after approximately 60 s. Thus, it can be observed that the functionalization applied to the membranes did not modify the oil wettability behavior of the surface, which remained superoleophilic. Moreover, the oleophilic properties of the PDMS-functionalized membranes were further confirmed by measuring the contact angle with various types of oils (i.e., silicone oil, soybean oil, and mineral oil). As shown in Fig. S4 of the Supporting Information, a final contact angle lower than 10° was obtained in all cases, confirming a consistent affinity between oils and the surface of the functionalized membranes. This behavior is particularly promising for practical membrane applications.

In view of the application of the membranes as oil/water separators, the liquid-liquid wettability of the EM-PDMS-5 %-1' functionalized system was also evaluated, measuring the contact angle of a drop of water on the membranes immersed in hexadecane (water-in-oil contact angle) and of a drop of hexadecane on the membranes immersed in water (oil-in-water contact angle). In the case of water-in-oil, a contact angle of 129° was recorded, as shown in Fig. 5a, confirming a highly hydrophobic behavior. This result is particularly interesting as it reproduces the actual condition of the membrane during application: the

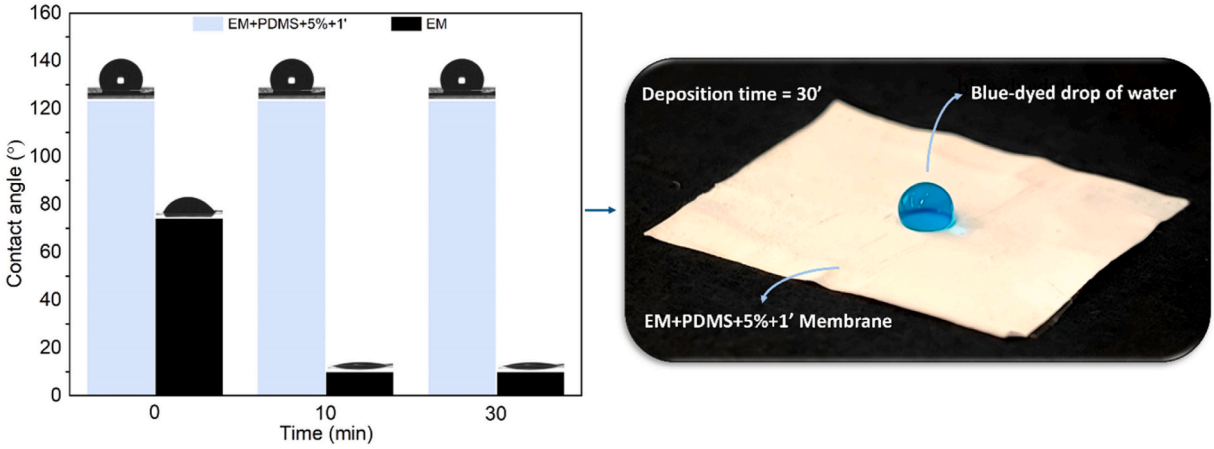

Fig. 4. Water contact angle of EM and EM-PDMS-5 %-1′ over time.

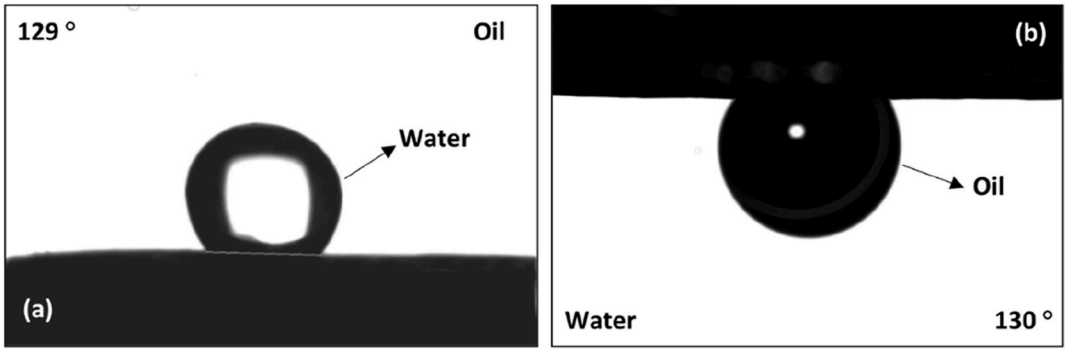

Fig. 5. (a) Water-in-oil contact angle and (b) oil-in-water contact angle for the EM-PDMS-5 %-1′ functionalized membrane.

membrane will be completely wet by the oil that passes through it and needs to retain water preventing its transfer. The stability of the water-in-oil contact angle was assessed: the contact angle did not vary over 4 h (remaining equal to 129°) and reached a value of 122° after 24 h, which is still within the range of hydrophobic performance.

In the case of oil-in-water, a contact angle of 130° was obtained, as shown in Fig. 5b. This result can be explained considering that the membrane was first immersed in water and then a drop of oil was deposited on its surface. Being hydrophobic, when immersed in water, the repulsive forces created a barrier effect preventing the oil from interacting directly with the membrane surface. Therefore, the value of the oil-in-water contact angle does not reflect the oleophilicity of the membrane, but rather the interactions between water and oil and the difference between the surface tension of both liquids. In fact, hydrophobic/oleophilic surfaces reliably perform their oil/water separation function as long as they encounter the oil phase during the separation process [8]. The oil-in-water contact angle did not show any variation after 24 h, presenting the same value of 130°.

The nanofibrous morphology of the electrospun mats, prior and after functionalization, was analyzed by FE-SEM technique. As shown in Fig. 6, the fibrous structure could be observed both before and after the photo-induced grafting, demonstrating that the processes did not affect the stability of the nanofibrous membranes. The fibers appeared as well-defined, cylindrical, uniform and continuous, forming a nonwoven mat with a high specific surface area.

Furthermore, the EM membranes (i.e., SBR membranes after electrospinning, photo-induced crosslinking and water treatment to remove the PEO polymeric template) displayed a peculiar surface nanostructure with high surface area, with the fibers composed of distinct rubber nanoparticles partially fused together (Fig. 6a and b), with an average diameter of 101.31 ± 0.61 nm. Likewise, the EM-PDMS-5 %-1' membranes consist of randomly distributed fibers formed by clearly distinguishable SBR particles with an average diameter of 101.32 ± 0.74 nm, as shown in Fig. 6e and f. The fact that the rubber nanoparticles did not change shape nor dimensions after the functionalization process confirmed the efficient stabilization of the SBR system by photo-crosslinking.

The functionalization of the membranes was further confirmed by elemental analysis using EDX spectroscopy. As shown in the spectrum of Fig. 6c for the EM sample, carbon, oxygen, and sulfur, which are the main elements of the crosslinked polymer network, are clearly detected. A small aluminum peak is also visible, originating from the substrate used to collect the electrospun membrane. In the EM-PDMS-5 %-1' sample (Fig. 6g), a significant presence of silicon, which derives from the PDMS grafting molecule, is observed. Notably, the spatial distribution of Si is highly uniform across the nanofibrous membrane, as illustrated in Fig. S5 of the Supporting Information.

The FE-SEM images were then analyzed to evaluate the mean diameter of the fibers as well as the distribution of the diameters within the membranes. An average fiber diameter of 638.2 ± 5.3 nm and of 438.97 ± 8.5 nm was obtained for EM and EM-PDMS-5 %-1′ samples, respectively. Similarly, the fiber diameter distribution also varied after treatment. The EM system showed a narrower fiber diameter distribution with respect to the EM-PDMS-5 %-1' system, as shown in Fig. 6d and h, confirming the effect of the functionalization process on the electrospun membrane. Indeed, after PDMS grafting, it was possible to observe a decrease in the regularity of the single fibers, which could be due to the action of the solvent (toluene) used to dilute the functionalizing monomer. However, the integrity and the porous structure of the membrane was preserved, and the surface of the SBR nanoparticles was mostly exposed, showing a very interesting morphology from the point of view of the potential filtering action of the membrane.

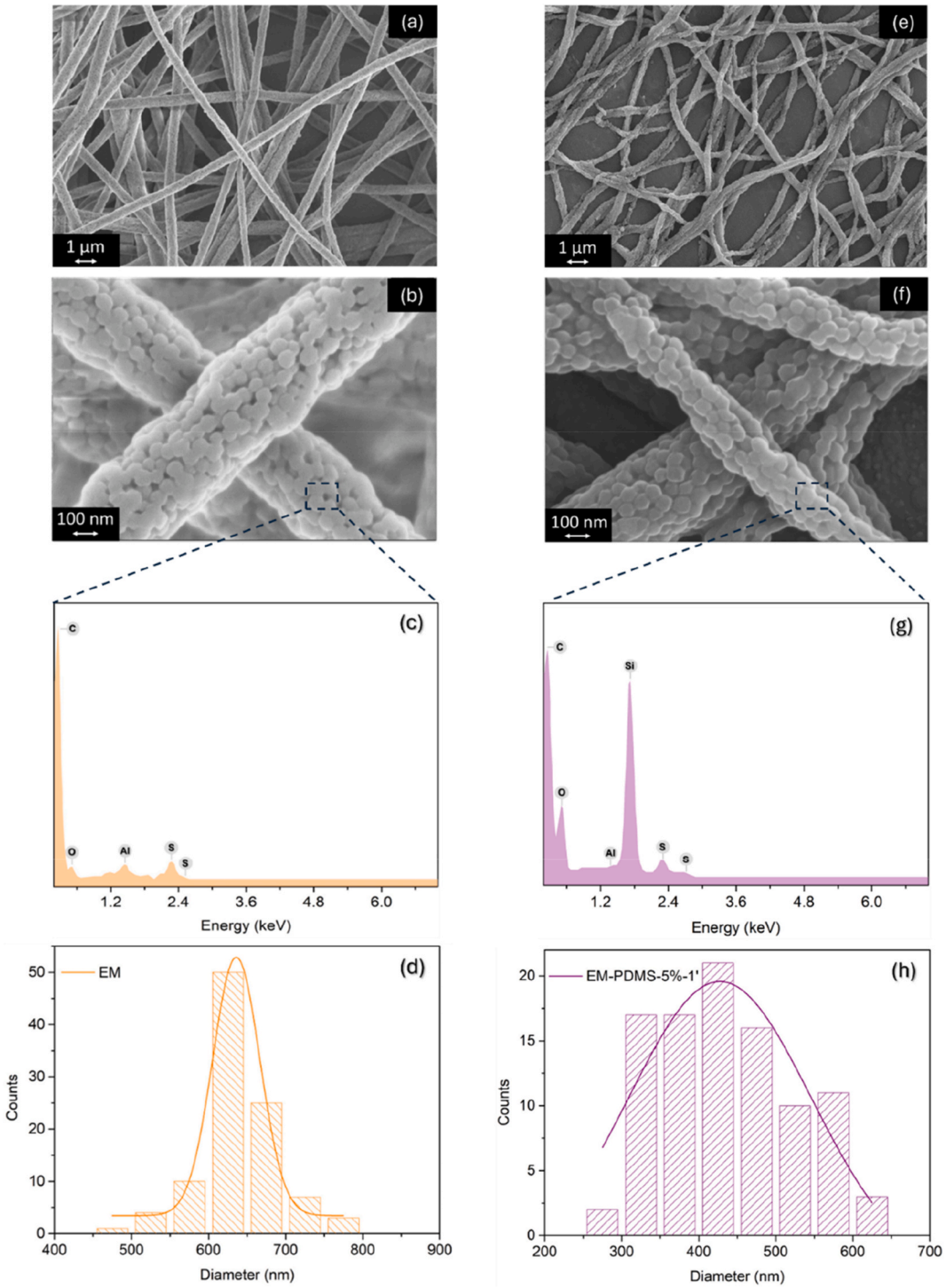

Fig. 6. Nanofibrous morphology: FE-SEM images of EM sample (a, b) and EM-PDMS-5 %-1′ sample (e, f), EDX spectra (c and g, respectively) and fiber diameter distribution (d and h, respectively).

Furthermore, FE-SEM images provided additional information on the surface porosity and average pore area, corresponding to the dimensions of the interfibrous gaps, of the PDMS-grafted membranes. These were found to be approximately 35 % and 0.80 μm^2, respectively, suggesting that the membrane can provide efficient separation performance while maintaining adequate fluid permeability. Thus, the nanostructured morphology, the stability of the system and the wettability behavior of the membranes represent interesting results regarding the application for the treatment of oil/water mixtures.

3.2. Performance of the PDMS-functionalized electrospun membranes in oil/water filtration processes

Given the results of the different characterization tests, the potential of SBR electrospun membranes as filtration systems for oil/water mixtures was studied. For this purpose, the penetration capacity of oil (hexadecane) and distilled water was tested. The test was performed by individually pouring each liquid into a simple filtration device (see Fig. S2 of the Supporting Information) containing either the reference membrane (EM) or the PDMS-grafted membrane exhibiting

hydrophobic/oleophilic properties (EM-PDMS-5 %-1′). Specifically, 5 mL of liquid were poured quickly, and the penetration capacity was assessed without applying any pressure for up to 30 min: the volume and weight of the liquid collected in the flask (i.e., that passed through the membrane) were monitored. Both liquids flowed efficiently and rapidly through the EM membrane, with weight penetration percentages of 99.9 ± 0.1 % for hexadecane and 99.4 ± 0.5 % for water. In contrast, for the EM-PDMS-5 %-1' membrane, oil readily penetrated (99.9 ± 0.1 % weight penetration), while water was entirely retained (0 % penetration).

The membranes' ability to separate oil and water was evaluated using the same method by quickly pouring a 1:1 volumetric mixture of both liquids. Specifically, 5 mL of oil (hexadecane) and 5 mL of dyed water were used, and liquid penetration was measured. For the reference EM membrane, both liquids immediately passed through upon pouring, driven solely by gravity, and mixed in the flask forming the permeate (Fig. 7a). This result confirmed that the membrane did not provide effective oil/water separation. In contrast, the EM-PDMS-5 %-1′ membrane allowed hexadecane to pass through while completely blocking water (Fig. 7b). The retained water remained suspended in the graduated cylinder due to the membrane's selective permeability. The system was left undisturbed for 1 h, during which no changes were observed, and no presence of water droplets was detected in the flask.

As illustrated in Fig. 7c, the filtration capacity of the membranes is conferred by the hydrophobic behavior achieved through PDMS surface grafting. This surface modification lowers the surface energy and increases water repellency, facilitating selective permeability and thereby improving the membrane efficiency in separating water from hydrophobic substances. Furthermore, gravitational force creates a pressure difference (ΔP) across the membrane which is sufficient to allow the liquid mixture to pass through it, eliminating the need for any externally applied pressure to achieve separation. These findings demonstrate that the PDMS-grafted rubber mats hold strong potential as materials for oil/water filtration membranes.

To further assess the oil/water separation performance of the PDMS-grafted membrane, the permeate fraction was left exposed to the open air overnight to allow any residual water to evaporate, and then its volume and weight were measured. The EM-PDMS-5 %-1' membrane exhibited an oil flux (φ) of 993.2 L m^{-2} h^{-1} and a separation efficiency (η) of 99.8 %. These values are competitive compared to other membranes reported in the literature for oil/water mixture and emulsion filtration [36–38].

To validate the consistency of these results, multiple filtration cycles (up to 20) were conducted using the same membrane. Each cycle involved alternately pouring 5 mL of hexadecane and 5 mL of dyed water into the filtration system and allowing the mixture to sit for 15 min. At the end of each cycle, the permeate and retentate were weighed, and their volumes were recorded. The separation efficiency and oil flux results for each cycle, presented in Fig. 8, confirm the stable performance of the functionalized SBR membranes. In particular, after 20 filtration cycles, a separation efficiency value of 99.3 % was obtained, while the average oil flux was 988.4 L m^{-2} h^{-1}. Although a slight

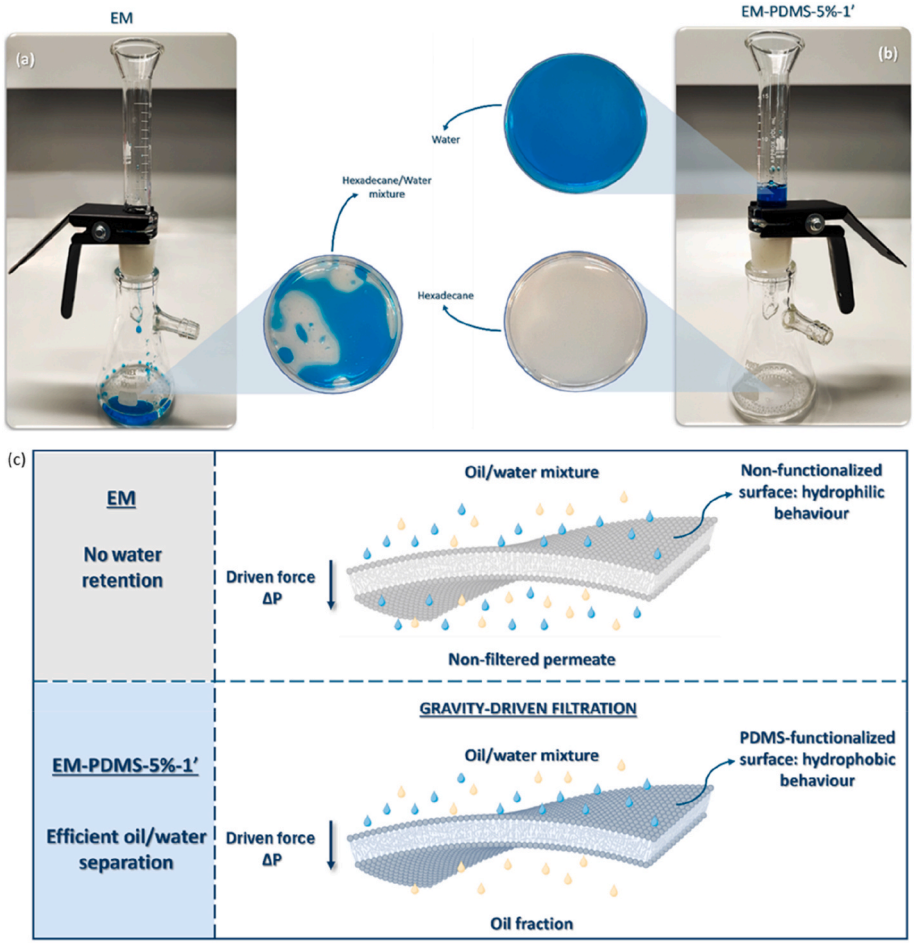

Fig. 7. Evaluation of the separation capacity of the membranes by using a 1:1 v/v mixture of dyed water and hexadecane. (a) Filtration by using the EM sample, and picture of the permeate mixture obtained after the test. (b) Filtration by using the EM-PDMS-5 %-1′ sample, showing the permeation of hexadecane and the retention of dyed water in the graduated cylinder. The picture represents the filtration system after 60 min. The separated water and hexadecane obtained through the filtration set-up are shown. (c) Scheme of the oil/water separation mechanism of an oil/water mixture using EM and EM-PDMS-5 %-1′ membranes.

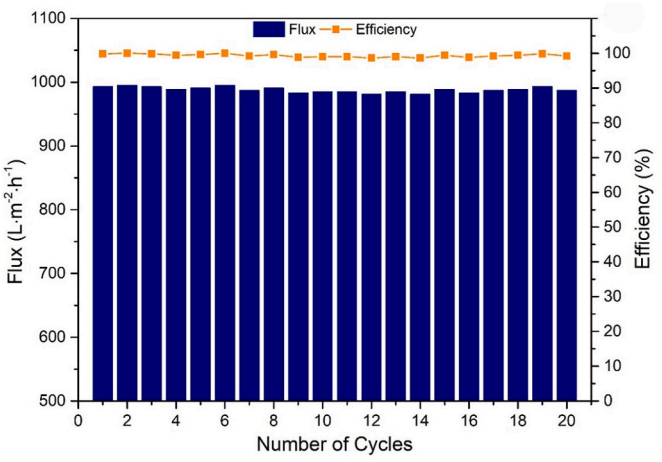

Fig. 8. Oil flux and separation efficiency of an oil/water mixture using EM-PDMS-5 %-1′ membrane, as a function of number of filtration cycles.

variation was observed compared to the values obtained in a single cycle, the performance of the PDMS-functionalized rubber membranes remained high even after 20 cycles. The sustained oil flux and separation efficiency over multiple cycles suggest that SBR swelling of oil does not significantly affect the membranes morphology or porosity during use. Further investigation to understand the causes of the minor reduction in oil flux and separation efficiency would be valuable, taking into account the need to optimize the filtration test procedure, controlling the potential slight solubility of oil in water, and checking possible membrane fouling effects. However, at the end of the test (i.e., after 20 filtration cycles), the filtration system was disassembled, and the structural integrity of the membrane was confirmed. Performance stability was further verified by measuring the contact angles of the used membrane in air, which remained at 123° for water and 8° for hexadecane. These results confirm the durability of the chemically grafted coating, which maintains stable hydrophobic and oleophilic properties even after prolonged use.

Table 2
Comparison of hydrophobic and oleophilic electrospun membranes for oil/water separation considering flux, efficiency and number of filtration cycles.

System	Flux ($L \cdot m^{-2} \cdot h^{-1}$)	Separation efficiency (%)	Number of filtration cycles	Reference
PDMS-functionalized membranes	988.4	99.3	20	This work
Polycaprolactone (PCL)/sulfonated lignin (SKL) membranes	170–480	>99	10	[39]
Sugarcane bagasse ester membranes	419.8	99.54	Multiple	[40]
Beeswax/PCL superhydrophobic membranes	1599	98	15	[41]
Polyvinilidene fluoride (PVDF)– fluorinated random copolymer (FCP) blend superhydrophobic membranes	1100	>99	Multiple	[42]
Superhydrophobic polypropylene (PP) membranes	685	99	10	[43]
PVDF–F-SiO_2 membrane	<1000	99.2	5	[44]
PDMS-PVDF membranes	848	98.7	10	[45]

Compared to other electrospun hydrophobic and oleophilic membranes reported in the literature (see Table 2) [39–45], the proposed system demonstrates superior or comparable flux and separation efficiency, often accompanied by significantly higher durability. Many existing membranes achieve either lower flux, reduced efficiency, or limited, and some require more complex fabrication processes. In contrast, the simple and versatile fabrication of the functionalized SBR membranes, along with their robust performance, underscores their strong potential as an effective solution for practical oil/water separation applications.

Finally, separation tests with EM-PDMS-5 %-1' membranes were performed using an oil-in-water emulsion. In this case, the separation process was slower (approximately twice the time compared to the case of filtration of the simple mixture), due to required diffusion of oil droplets, allowing the difference in density between water and hexadecane to partially establish the separation of the mixture in the graduated cylinder. However, it was shown that the membrane was able to efficiently separate the emulsion as well. Both the permeate and the concentrate fractions were individually observed through optical microscope to evaluate the separation process from a qualitative point of view. An efficient separation of the emulsion was obtained: as shown in Fig. S6 of the Supporting Information, both water and hexadecane were clear, and no tiny droplets of the other liquid were detected. In the case of filtration of the emulsion, the separation efficiency was 99.4 %, which is comparable to the percentage obtained in the case of the simple mixture. However, being the filtration a slower process, the oil flux obtained was considerably lower, with a value of 529.9 L m^{-2} h^{-1}.

4. Conclusions

This study presents a simple and rapid method for preparing rubber nanofibrous membranes via suspension electrospinning of SBR latex, followed by photo-induced crosslinking and photo-induced grafting to achieve morphological stability and permanent hydrophobicity and oleophilicity. Specifically, a vinyl-terminated PDMS functionalizing agent was grafted onto the nanofibers through a thiol-ene reaction, under different functionalization conditions (i.e., varying solution concentrations and immersion times). The optimal grafting parameters were determined to be a PDMS concentration of 5 wt% and an immersion time of 1 min. FT-IR analyses confirmed the successful functionalization of the membranes. The resulting PDMS-grafted electrospun fibers were well-defined, cylindrical, uniform, and continuous, exhibiting a distinctive nanostructured surface with a high surface area, composed of partially fused rubber nanoparticles. The functionalization process, conducted in toluene, led to a slight decrease in the average fibers diameter, which measured 439 nm for the PDMS-grafted membranes. Contact angle tests demonstrated that the developed PDMS-functionalized rubber nanofibrous membranes maintained their hydrophobicity over time (water contact angle of 123.4° after 30 min and water-in-oil contact angle of 121.9° after 24 h), while exhibiting pronounced oleophilicity (oil contact angle <10°). Additionally, the membranes effectively separated oil from water, achieving an average separation efficiency of 99.3 % and an oil flux of 988.4 L m^{-2} h^{-1} after 20 filtration cycles of an oil/water mixture. When tested with an oil-in-water emulsion the membranes demonstrated a separation efficiency of 99.4 % and an oil flux of 529.9 L m^{-2} h^{-1}. The successful oil/water separation results highlight the significant potential of the developed hydrophobic/oleophilic PDMS-functionalized rubber nanofibrous membranes for the treatment of oily wastewater and environmental remediation applications.

CRediT authorship contribution statement

Jessica Alexandra Talamo Ruiz: Writing – original draft, Visualization, Validation, Methodology, Investigation. **Parnian Kianfar:** Methodology, Investigation, Conceptualization. **Sara Dalle Vacche:**

Writing – review & editing, Investigation. **Roberta Bongiovanni:** Writing – review & editing, Resources, Funding acquisition. **Alessandra Vitale:** Writing – review & editing, Visualization, Supervision, Resources, Project administration, Funding acquisition, Conceptualization.

Declaration of competing interest

The authors declare that they have no known competing financial interests or personal relationships that could have appeared to influence the work reported in this paper.

Acknowledgments

The authors acknowledge RESCOM srl for kindly providing the SBR latex. One of the coauthors (R.B.) acknowledges support by the Italian Ministry of Foreign Affairs and International Cooperation, grant number EG24GR02.

Appendix A. Supplementary data

Supplementary data to this article can be found online at https://doi.org/10.1016/j.memsci.2025.124457.

Data availability

Data will be made available on request.

References

[1] Y. Wei, H. Qi, X. Gong, S. Zhao, Specially wettable membranes for oil–water separation, Adv. Mater. Interfac. 5 (23) (2018) 1800576, https://doi.org/10.1002/admi.201800576.
[2] L. Yu, M. Han, F. He, A review of treating oily wastewater, Arab. J. Chem. 10 (2017) S1913–S1922, https://doi.org/10.1016/j.arabjc.2013.07.020.
[3] K. Abuhasel, M. Kchaou, M. Alquraish, Y. Munusamy, Y.T. Jeng, Oily wastewater treatment: overview of conventional and modern methods, challenges, and future opportunities, Water 13 (7) (2021) 980, https://doi.org/10.3390/w13070980.
[4] A.D. M.d. Medeiros, C.J. G.d. Silva Junior, J.D. P.d. Amorim, I.J.B. Durval, A.F.d. S. Costa, L.A. Sarubbo, Oily wastewater treatment: methods, challenges, and trends, Processes 10 (4) (2022) 743, https://doi.org/10.3390/pr10040743.
[5] T.V. Le, T. Imai, T. Higuchi, K. Yamamoto, M. Sekine, R. Doi, H.T. Vo, J. Wei, Performance of tiny microbubbles enhanced with “normal cyclone bubbles” in separation of fine oil-in-water emulsions, Chem. Eng. Sci. 94 (2013) 1–6, https://doi.org/10.1016/j.ces.2013.02.044.
[6] M. Han, J. Zhang, W. Chu, J. Chen, G. Zhou, Research progress and prospects of marine oily wastewater treatment: a review, Water 11 (12) (2019) 2517, https://doi.org/10.3390/w11122517.
[7] M.R.G. Santos, M.O.F. Goulart, J. Tonholo, C.L.P.S. Zanta, The application of electrochemical technology to the remediation of oily wastewater, Chemosphere 64 (3) (2006) 393–399, https://doi.org/10.1016/j.chemosphere.2005.12.036.
[8] P. Sahoo, A.A. Ramachandran, P.K. Sow, A comprehensive review of fundamentals and future trajectories in oil-water separation system designs with superwetting materials, J. Environ. Manag. 370 (2024) 122641, https://doi.org/10.1016/j.jenvman.2024.122641.
[9] G. Kwon, E. Post, A. Tuteja, Membranes with selective wettability for the separation of oil–water mixtures, MRS Commun. 5 (3) (2015) 475–494, https://doi.org/10.1557/mrc.2015.61.
[10] S. Rasouli, N. Rezaei, H. Hamedi, S. Zendehboudi, X. Duan, Superhydrophobic and superoleophilic membranes for oil-water separation application: a comprehensive review, Mater. Des. 204 (2021) 109599, https://doi.org/10.1016/j.matdes.2021.109599.
[11] N. Baig, M. Sajid, B. Salhi, I. Abdulazeez, Special wettable membranes for oil/water separations: a brief overview of properties, types, and recent progress, Colloids and Interfaces 7 (1) (2023) 11, https://doi.org/10.3390/colloids7010011.
[12] J. Wendorff, M. Burgard, A. Greiner, S. Agarwal, Electrospinning: a Practical Guide to Nanofibers, De Gruyter, 2016, https://doi.org/10.1515/9783110333510.
[13] A. Keirouz, Z. Wang, V.S. Reddy, Z.K. Nagy, P. Vass, M. Buzgo, S. Ramakrishna, N. Radacsi, The history of electrospinning: past, present, and future developments, Advanced Materials Technologies (2023), https://doi.org/10.1002/admt.202201723.
[14] S. Agarwal, A. e Greiner, J.H. Wendorff, Functional materials by electrospinning of polymers, Prog. Polym. Sci. 38 (6) (2013) 963–991, https://doi.org/10.1016/j.progpolymsci.2013.02.001.
[15] G.B. Medeiros, F.d.A. Lima, D.S. de Almeida, V.G. Guerra, M.L. Aguiar, Modification and functionalization of fibers formed by electrospinning: a review, Membranes 12 (9) (2022) 861, https://doi.org/10.3390/membranes12090861.
[16] X. Yan, X. Xiao, C. Au, S. Mathur, L. Huang, Y. Wang, Z. Zhang, Z. Zhu, M. Kipper, J. Tang, J. Chen, Electrospinning nanofibers and nanomembranes for oil/water separation, J. Mater. Chem. A (2021), https://doi.org/10.1039/d1ta05873h.
[17] Y. Liao, C.-H. Loh, M. Tian, R. Wang, A.G. Fane, Progress in electrospun polymeric nanofibrous membranes for water treatment: fabrication, modification and applications, Prog. Polym. Sci. 77 (2018) 69–94, https://doi.org/10.1016/j.progpolymsci.2017.10.003.
[18] Y. Li, X. Wang, Z. Peng, P. Li, C. Li, L. Kong, Fabrication and properties of elastic fibers from electrospinning natural rubber, J. Appl. Polym. Sci. 136 (43) (2019) 48153, https://doi.org/10.1002/app.48153.
[19] Y. Tertyshnaya, S. Karpova, M. Moskovskiy, A. Dorokhov, Electrospun polylactide/natural rubber fibers: effect natural rubber content on fiber morphology and properties, Polymers 13 (14) (2021) 2232, https://doi.org/10.3390/polym13142232.
[20] H.C. Duong, D. Chuai, Y.C. Woo, H.K. Shon, L.D. Nghiem, V. Sencadas, A novel electrospun, hydrophobic, and elastomeric styrene-butadiene-styrene membrane for membrane distillation applications, J. Membr. Sci. 549 (2018) 420–427, https://doi.org/10.1016/j.memsci.2017.12.024.
[21] J. Yoon, J. Lee, J. Hur, Stretchable supercapacitors based on carbon nanotubes-deposited rubber polymer nanofibers electrodes with high tolerance against strain, Nanomaterials 8 (7) (2018) 541, https://doi.org/10.3390/nano8070541.
[22] P. Kianfar, A. Bakry, S. Dalle Vacche, R. Bongiovanni, A. Vitale, Suspension electrospinning of SBR latex combined with photo-induced crosslinking: control of nanofiber composition, morphology, and properties, J. Mater. Sci. 59 (2024) 3711–3724, https://doi.org/10.1007/s10853-024-09416-8.
[23] J. Cui, T. Lu, F. Li, Y. Wang, J. Lei, W. Ma, Y. Zou, C. Huang, Flexible and transparent composite nanofibre membrane that was fabricated via a “green” electrospinning method for efficient particulate matter 2.5 capture, J. Colloid Interface Sci. 582 (2021) 506–514, https://doi.org/10.1016/j.jcis.2020.08.075.
[24] A. Vitale, G. Massaglia, A. Chiodoni, R. Bongiovanni, C.F. Pirri, M. Quaglio, Tuning porosity and functionality of electrospun rubber nanofiber mats by photo-crosslinking, ACS Appl. Mater. Interfaces 11 (27) (2019) 24544–24551, https://doi.org/10.1021/acsami.9b04599.
[25] C. Hoyle, C. Bowman, Thiol–ene click chemistry, Angew. Chem. Int. Ed. 49 (2010) 1540–1573, https://doi.org/10.1002/anie.200903924.
[26] W. Yu, X. Lu, L. Xiong, J. Teng, C. Chen, B. Li, B.-Q. Liao, H. Lin, L. Shen, Thiol-ene click reaction in constructing liquid separation membranes for water treatment, Small 20 (2024) 2310799, https://doi.org/10.1002/smll.202310799.
[27] J. Hu, S. Yuan, W. Zhao, C. Li, P. Liu, X. Shen, Fabrication of a superhydrophilic/underwater superoleophobic PVDF membrane via thiol–ene photochemistry for the oil/water separation, Colloids Surf. A Physicochem. Eng. Asp. 664 (2023) 131138, https://doi.org/10.1016/j.colsurfa.2023.131138.
[28] E.J. Park, W.H. Lee, C. Bae, Versatile functionalization of aromatic polysulfones via thiol-ene click chemistry, J. Polym. Sci. Polym. Chem. 54 (19) (2016) 3237–3243, https://doi.org/10.1002/pola.28210.
[29] X. Wang, X. Feng, Q. Li, Z. Dong, Surface functionalization strategy for cellulose membranes based on silanization and thiol–ene click chemistry, ACS Appl. Polym. Mater. 6 (21) (2024) 12992–13001, https://doi.org/10.1021/acsapm.4c01842.
[30] M. Zhu, Y. Liu, A. Rahimpour, Y. Liu, M. Sadrzadeh, Fabrication of fluorine-free pH-responsive functionalized mesh via thiol-ene click chemistry for oil-water separation, Surf. Coating. Technol. 470 (2023) 129792, https://doi.org/10.1016/j.surfcoat.2023.129792.
[31] H. Liu, D. Wang, H. Huang, W. Zhou, Z. Chu, Cysteine-based antifouling superhydrophilic membranes prepared via facile thiol-ene click chemistry for efficient oil-water separation, J. Environ. Chem. Eng. 12 (3) (2024) 112654, https://doi.org/10.1016/j.jece.2024.112654.
[32] B. Shen, C. Du, W. Wang, D. Yu, Antifouling hydrophilic electrostatic spinning PAN membrane based on click chemistry with high efficiency oil-water separation, Fibers Polym. 23 (12) (2022) 3386–3397, https://doi.org/10.1007/s12221-022-4095-2.
[33] L. Tian, G. Ren, P. Zhang, B. Li, S. Chang, H. Yu, R. Wang, J. He, Preparation of fluorine-free waterproof and breathable electrospun nanofibrous membranes via thiol-ene click reaction, Macromol. Mater. Eng. 307 (4) (2022) 2100757, https://doi.org/10.1002/mame.202100757.
[34] J. Zhou, A.V. Ellis, N.H. Voelcker, Recent developments in PDMS surface modification for microfluidic devices, Electrophoresis 31 (1) (2010) 2–16, https://doi.org/10.1002/elps.200900475.
[35] C.F. Carlborg, T. Haraldsson, K. Öberg, M. Malkoch, W. van der Wijngaart, Beyond PDMS: off-stoichiometry thiol–ene (OSTE) based soft lithography for rapid prototyping of microfluidic devices, Lab Chip 11 (18) (2011) 3136, https://doi.org/10.1039/c1lc20388f.
[36] W. Zhang, Z. Shi, F. Zhang, X. Liu, J. Jin, L. Jiang, Superhydrophobic and superoleophilic PVDF membranes for effective separation of water-in-oil emulsions with high flux, Adv. Mater. 25 (14) (2013) 2071–2076, https://doi.org/10.1002/adma.201204520.
[37] S. Jiang, X. Meng, B. Chen, N. Wang, G. Chen, Electrospinning superhydrophobic–superoleophilic PVDF-SiO 2 nanofibers membrane for oil–water separation, J. Appl. Polym. Sci. 137 (47) (2020) 49546, https://doi.org/10.1002/app.49546.
[38] W. Ma, M. Zhang, Z. Liu, M. Kang, C. Huang, G. Fu, Fabrication of highly durable and robust superhydrophobic-superoleophilic nanofibrous membranes based on a fluorine-free system for efficient oil/water separation, J. Membr. Sci. 570–571 (2019) 303–313, https://doi.org/10.1016/j.memsci.2018.10.035.
[39] N.E.B. Surat’man, X.L. Quek, N. Wang, E. Ye, J. Xu, Z. Li, B. Li, Sustainable nanofibrous membranes for air filtration, water purification and oil removal, Nanoscale 17 (2025) 6427–6447, https://doi.org/10.1039/d4nr04673k.

[40] W. Chen, H. Wang, W. Lan, A. Zhang, C. Liu, Fabrication of sugarcane bagasse ester-based porous nanofiber membrane by electrospinning for efficient oil-water separation, Ind. Crop. Prod. 187 (2022) 115480, https://doi.org/10.1016/j.indcrop.2022.115480.

[41] C.R. Reshmi, S.P.A.J. Sundaran, S. Athiyanathil, Fabrication of superhydrophobic polycaprolactone/beeswax electrospun membranes for high-efficiency oil/water separation, RSC Adv. 7 (4) (2017) 2092–2102, https://doi.org/10.1039/c6ra26123j.

[42] I. Sadeghi, N. Govinna, P. Cebe, A. Asatekin, Superoleophilic, mechanically strong electrospun membranes for fast and efficient gravity-driven oil/water separation, ACS Appl. Polym. Mater. 1 (4) (2019) 765–776, https://doi.org/10.1021/acsapm.8b00279.

[43] A.M. Kansara, S.G. Chaudhri, P.S. Singh, A facile one-step preparation method of recyclable superhydrophobic polypropylene membrane for oil–water separation, RSC Adv. 6 (66) (2016) 61129–61136, https://doi.org/10.1039/c6ra11008h.

[44] Y. Yang, Y. Li, L. Cao, Y. Wang, L. Li, W. Li, Electrospun PVDF-SiO2 nanofibrous membranes with enhanced surface roughness for oil-water coalescence separation, Separ. Purif. Technol. 269 (2021) 118726, https://doi.org/10.1016/j.seppur.2021.118726.

[45] J. Li, Y. Li, Y. Lu, W. Shi, H. Tian, PDMS/PVDF electrospinning membranes for water-in-oil emulsion separation and UV protection, Biomimetics 7 (4) (2022) 217, https://doi.org/10.3390/biomimetics7040217.